# A general purpose LES Model for Atomization

Javier Anez, François Xavier Demoulin, Nicolas Hecht, Julien Reveillon

▶ **To cite this version:**

Javier Anez, François Xavier Demoulin, Nicolas Hecht, Julien Reveillon. A general purpose LES Model for Atomization. European Conference Liquid Atomization & Spray Systems, Sep 2016, Brighton, United Kingdom. hal-02128542

**HAL Id: hal-02128542**
**https://hal.science/hal-02128542v1**

Submitted on 14 May 2019

**HAL** is a multi-disciplinary open access archive for the deposit and dissemination of scientific research documents, whether they are published or not. The documents may come from teaching and research institutions in France or abroad, or from public or private research centers.

L'archive ouverte pluridisciplinaire **HAL**, est destinée au dépôt et à la diffusion de documents scientifiques de niveau recherche, publiés ou non, émanant des établissements d'enseignement et de recherche français ou étrangers, des laboratoires publics ou privés.

# A general purpose LES Model for Atomization

Javier Anez, François Xavier Demoulin*, Nicolas Hecht, Julien Reveillon.
Department of Turbulence, Atomization, Spray and Chaos, CORIA UMR 6614, Rouen, France
*Corresponding author: demoulin@coria.fr

**Abstract**
Several approaches have been used to simulate liquid jet atomization phenomena. Usually a modeling strategy is assumed for liquid jet morphology, interface capturing methods are used for primary atomization while dispersed methods such as Lagrangian particle-tracking approach may be used to model the final spray. Despite recent developments in numerical methods and computer performance, complete simulation of atomization and spray remains inaccessible for practical applications (e.g. Diesel/Gasoline injectors, Feedstock atomization on FCC riser reactors, among others). Therefore, an enhanced Euler-Lagrange Spray Atomization (ELSA) approach to the well-established LES turbulence model merged with an interface density equation for subgrid scales is introduced. Moreover, the method has been adapted for unstructured mesh within OpenFOAM framework. Furthermore, a coupling with Lagrangian particle tracking has been performed. Several validation stages are being tested by comparing experimental data (i.e. ECN Spray injectors) and DNS results against the proposed model. Finally, an industrial application case using a FCC injector® demonstrates the suitability of this novel model, based on good quantitative and qualitative agreement with experiments and DNS simulations.

**Introduction**
Fluid Catalytic Cracking (FCC) is a process where the crude oil is transformed into Gasoline, olefins and distillates. In this process, the liquid oil feed is atomized through a set of injectors connected circumferentially to a riser. Moreover, the oil droplets are vaporized and cracked within the riser upon contacting hot gases and catalyst, respectively [1]. The main goal in an injector design is to produce small size droplets in order to ensure quick vaporization and intimate contact with the catalyst [2].

Most studies have assumed instant vaporization and uniform catalyst/oil ratio at the bottom of riser cross-sectional area, based on the assumption that the cracking time scale is much longer than the time scale of interface transport in the feed injection zone [3, 4]. Some studies considered the vaporization rate of the liquid oil using two approaches, namely homogeneous and heterogeneous mode, in which both methods set the limits for the actual vaporization time [5]. When it comes to FCC riser modeling many researchers have focused on the upper and middle zone of the riser and just a few researchers on nozzles and feed atomization zone [6], mainly due to the high constraints using multidimensional models with chemical reactions, vaporization, and atomization within an industrial scale. Theologos [7] studied atomization effects on reactor performance and found that smaller droplets produce higher vaporization rates. Therefore, the need for a deeper understanding of the physics and atomization mechanisms involved within a FCC injector coupled with the feed injection zone urged to be tackled. The aim of this project is to numerically model the oil-steam mixing inside the FCC injector.

**Material and methods**
The objective of this work is to extend LES-ELSA method [8] into a general purpose solver within OpenFOAM® framework. A postulated transport equation of the interface density is implemented to describe the subgrid spray formation from interface wrinkling, ligament breakup, sheets to the breakup droplets. The interface capturing method is based on the transport of a liquid volume fraction (i.e.$\alpha_l$). Accordingly, an additional compressive term is added to the equation to treat sharpened $\alpha_l$ gradients. In LES, a subgrid- scale (SGS) model accounts for the dynamics of the unresolved scales of motion which induces a subgrid scale (i.e.$SGS_{\alpha_l}$) that is not compatible with the numerical procedure used to capture the interface. The advantages of the proposed method is to disable the compressive term when $SGS_{\alpha_l}$ becomes important (i.e. when the interface fluctuations become significant at subgrid-scale). Two criterions are used to switch from interface capturing method to subgrid-scale or vice versa, based on Interface Resolution Quality (i.e. $IRQ$, which is derived from the transport equation of the interface density, ELSA algorithm).

In order to upgrade LES-ELSA method a coupling with Lagrangian particle was performed. Lagrangian particles are created when liquid structures become droplets. The diameter and the number of particle are determined via liquid volume fraction and via the interface density equation. The Eulerian model has been linked to the Lagrangian phase using the liquid turbulent diffusion flux closure.

**Numerical Model**

Atomization by definition is the process of converting a liquid form to a free gaseous atom. In other words, it is the transformation of a bulk liquid into a spray of liquid droplets in a surrounding gas or vacuum [9]. Three different zones can be easily defined as shown in figure 1. The first region near the tip of the injector is called primary atomization. In this area the liquid volume fraction is close to one and the liquid surface topology is very complex. Here the liquid sheets experience longitudinal instabilities based on liquid and gas interactions (Kelvin-Helmholtz instabilities) which disturb the plane sheet in a sinusoidal stream-wise oscillation mode. the secondary atomization begins downstream of the flow, where instabilities turn into three dimensions, and the sheet breaks into smaller liquid packs, ligaments and bag-like structures. This zone ends with the formation of a spray of droplets (Dispersed zone) [11].

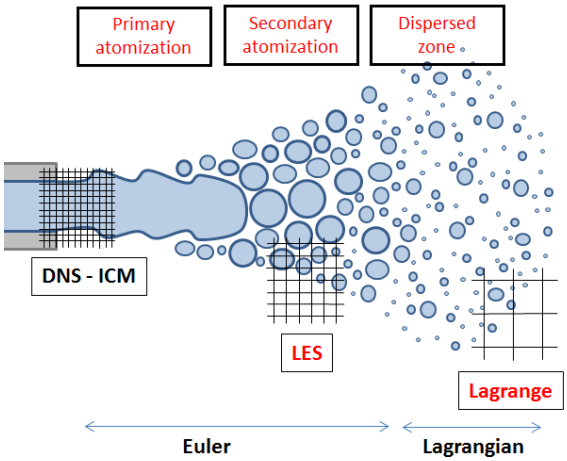


**Figure 1.** Atomization zones. Source: [10]

The ELSA model, which is devoted to describe atomization flows with high Weber and Reynolds values, has been adapted to account for both primary and secondary atomization zone by using an Euler approach. In this model the two phase flow is considered as single phase flow composed of two species, liquid and gas, with highly variable density [12, 13]. The dispersion of the liquid phase is calculated by a liquid volume fraction balance equation ($\alpha_l$) using a pondered inclusion of a 'turbulent diffusion liquid flux' [10] and interface capturing method (ICM) used in OpenFOAM®, as shown in equation 1. Such ponderation is ruled by an arbitrary parameter ($C_\alpha$) which depends on the interface resolution scale.

$$\frac{\partial \alpha_1}{\partial t} + \frac{\partial u_j \alpha_1}{\partial x_j} + \underbrace{\frac{\partial C_\alpha u_{rj} \alpha_1 (1-\alpha_1)}{\partial x_j}}_{\text{ICM}} = 0 + \underbrace{(1- C_\alpha) \frac{\partial S_{sb\alpha_1}}{\partial x_j}}_{\text{Subgrid ELSA-LES}} \quad (1)$$

The interface capturing method consists in defining an artificial and supplementary velocity field, ($u_r$), in the vicinity of the interface, in such a way that the local flow steepens the gradient of the volume fraction and the interface resolution is improved [14]. The turbulent diffusion flux represents the transport of the liquid volume fraction induced by velocity fluctuations as shown in equation 2 by analogy with Fick's law. [15]

$$\dot{S}_{sb\alpha_1} = \frac{\partial (\overline{u_j}.\overline{\alpha_1} - \overline{u_j \alpha_1})}{\partial x_j} = \frac{\nu_t}{Sch} \frac{\partial \overline{\alpha_1}}{\partial x_j} \quad (2)$$

Where '$\boldsymbol{Sch}$' is the Schmidt number. It is important to note that this approach is valid only in the absence of a mean slip velocity between the phases [13]. The arbitrary parameter ($C_\alpha$) was set zero when the interface is poor-resolved (Secondary atomization) and set to one otherwise (Primary atomization) as shown in figure 2. Two

criterions have been used to properly set, $C_\alpha$, based on the Interface Resolution Quality (i.e. $IRQ$, which is derived from the transport equation of the interface density [10]).


**Figure 2.** Ponderation parameter ($C_\alpha$). Source [10]

The breakup process and the polydisperse spray distribution are accounted through the quantity, $\bar{\Sigma}\,(m^{-1})$, mean interfacial area per unit of volume, as shown in equation 3.

$$\frac{\partial \bar{\Sigma}}{\partial t} + \frac{\partial \overline{u_j}\bar{\Sigma}}{\partial x_j} = \frac{\partial}{\partial x_j}\left(\frac{\nu_t}{Sch}\frac{\partial \bar{\Sigma}}{\partial x_j}\right) + \frac{\bar{\Sigma}}{\tau_t}\left(1 - \frac{\bar{\Sigma}}{\Sigma^*}\right) \tag{3}$$

The first criterion to define the weighted parameter, $C_\alpha$, is given by the ratio of the minimum (resolved) interface ($\frac{2{,}4\sqrt{\alpha(1-\alpha)}}{\Delta}$) over the actual interface calculated from $\bar{\Sigma}$ equation. It can be seen on figure 3-a, the higher the interface fluctuations, the lower $IRQ_\Sigma$, which means instabilities have turned into three dimensional effect and secondary atomization zone is considered. The second criterion is grid-dependant, especially if LES turbulence modelling is applied using as a cutoff width $\Delta$, *cubit root of the grid cell volume.* $IRQ_\kappa$, is defined taking into account the curvature of the interface, k. Figure 3-b displays the relationship between interface radius and cell size. The higher the interface radius, the better resolution of the interface, thus $C_\alpha$ is set to zero.

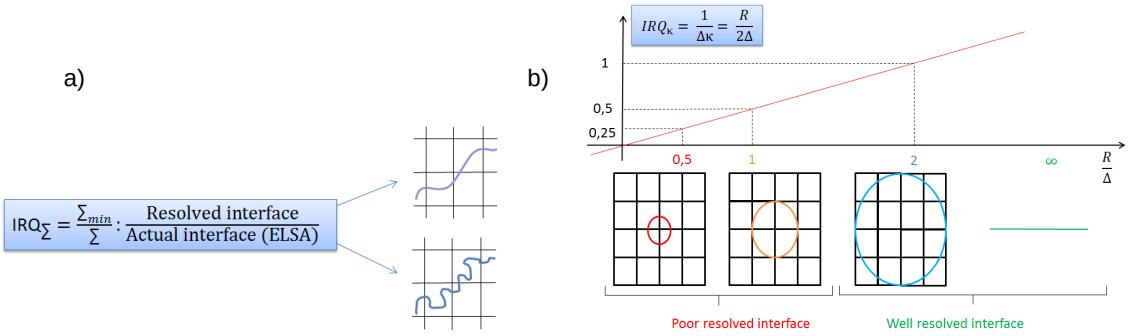


**Figure 3.** a) Interface resolution quality, $\bar{\Sigma}$. b) Interface resolution quality, $IRQ_\kappa$ (curvature resolution). Source: [10]

In this work, the two phases are assumed at constant density, $\rho$, so that turbulent fluctuations of mixture density $\rho'$ are only due to volume fraction, as displayed in equation 4.

$$\rho' = \rho_l \alpha_1' + \rho_g(1 - \alpha_1') \tag{4}$$

Finally the filtered unsteady Navier-Stokes equations are presented. Instead of time-averaging, LES uses a spatial filtering operation to separate the larger and smaller eddies [16]. In equation 6, the last term on RHS are the subgrid scale stresses, just like the Reynolds stresses in the RANS momentum equations that arise as a consequence of time-averaging.

$$\frac{\partial \bar{\rho}\,\overline{u_i}}{\partial t} + \frac{\partial \bar{\rho}\,\overline{u_j}\,\overline{u_i}}{\partial x_j} = \frac{\partial \bar{p}}{\partial x_j} + \frac{\partial}{\partial x_j}\left(\mu\frac{\partial \overline{u_i}}{\partial x_j}\right) + \frac{\partial \tau_{ij}}{\partial x_j}, \qquad \tau_{ij} = \overline{u_l u_j} - \overline{u_l}\,\overline{u_j} = -\mu_{sgs}\left(\frac{\partial \overline{u_i}}{\partial x_j} + \frac{\partial \overline{u_j}}{\partial x_i}\right) + \frac{1}{3}\tau_{ii}.\delta_{ij} \text{ (SGS Stresses)} \tag{5}$$

These stresses are modelled using Smagorinsky-Lilly SGS model which are taken to be proportional to the local rate of strain of the resolved flow. The Smagorinsky-Lilly model builds on Prandtl's mixing length model, and assumes that we can define a dynamic SGS viscosity, $\mu_{sgs}$, which can be described in terms of one length scale $\Delta$, and one velocity scale and it is related to the kinematic SGS viscosity $\nu_{sgs}$. As in the length mixing model, the velocity scale is expressed as the product of the length scale and the average strain rate of the resolved flow, $\Delta.|\bar{S}|$ [16], Thus, the SGS viscosity is evaluated as follows:

$$\mu_{sgs} = \rho(C_{sgs}\Delta)^2|\bar{S}| \quad (6)$$

It is worth mention that the previous variables such as liquid volume fraction, $\alpha$, and the mean interface area per unit of volume $\bar{\Sigma}$, were filtered as well, and the previous approach was implemented.

## Results and discussion

### Validation

Before proceeding and applying LES-ELSA-Lagrange model to the FCC oil injector is necessary first to validate the algorithm by means of the experimental dataset developed by the ECN Group (Engine Combustion Network). Specifications of the injector are detailed in figure 4-a. In this work the injector chamber was chosen and meshed using OpenFOAM®'s utility, *BlockMesh*. The mesh consists of 1.4 million un-structured hexahedral cells, as shown in figure 4-b and figure 4-c.

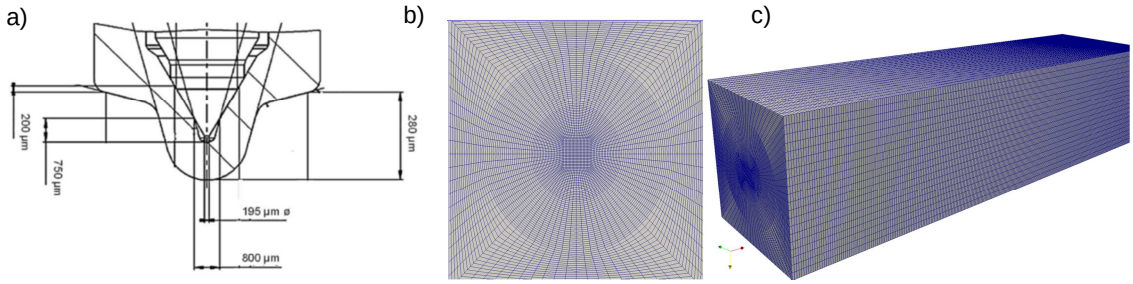


**Figure 4.** a) ECN injector geometry and dimensions. b) Mesh view at inlet plane of the injector. c) 3-D Mesh of the injection chamber. Source: [10]

Table 1 displays the liquid properties used to simulate the atomization process within the ECN injector chamber. In order to reach convergence and hence, get time-independent results, the liquid was allowed to cross four times the injector chamber completely in the axial direction.

**Table 1.** Liquid properties. Source [10]

| | Symbols | Value |
|---|---|---|
| Liquid Density | $\rho_l\ (kg.m^{-3})$ | 803 |
| Liquid Viscosity | $\mu_l(kg.\ m^{-1}s^{-1})$ | $3{,}2\text{x}10^{-03}$ |
| Surface Tension | $\sigma\ (N.m^{-1})$ | $2{,}54\text{x}\ 10^{-02}$ |

Once the results reach convergence, the liquid volume fraction is plotted on plane slice and as iso-surface coloured by velocity as displayed in figure 5-a, and figure 5-b, respectively. It can be seen on both pictures the difference between the resolved scale near the exit of the injector (inlet of the injector chamber) and the poorly-resolved scales downstream of the flow where the subgrid fluctuations become important. At the inlet there is a clear definition of the interface, thanks to the interface capturing method. On the other hand, downstream of the flow, the turbulent diffusion liquid flux dominates, and it is perceived the beginning of the mixing of the phases as the liquid volume fraction decreases. For validation purpose, two radial planes were located at 500 and 1500 microns from the inlet of the injector tip as displayed in figure 5-c, in order to calculate the surface liquid velocity, $(u_i|_\Sigma)$, as it moves away radially from the centerline of the injector.

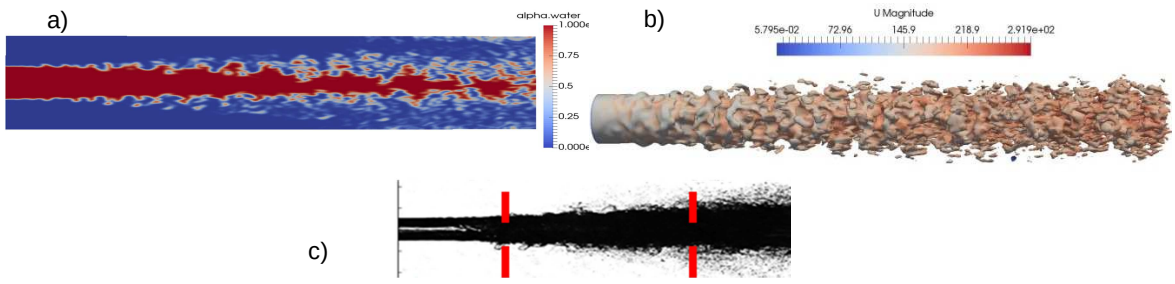


**Figure 5.** a) Liquid volume fraction. b) Iso-Surface of 0.5 liquid volume fraction coloured by Velocity. c) Radial probe planes located in longitudinal axis (source [17]).

Figure 6 exhibits the comparison of the averaged surface liquid velocity, $(u_i|_\Sigma)$, on the two radial planes highlighted above, from Experiments, DNS, New DNS, and ELSA-LES + Lagrange equation for droplets velocity. Firstly the difference between DNS and New DNS is based on how the convective term is solved in the volume fraction and momentum equations. Since the latter relies on the mixture density (equation 4), the momentum equation can be recast, so the exact convective term can also appear, plus additional terms. This convective term is treated differently for DNS cases. On the contrary, New DNS solves consistently [18]. Secondly the experimental results were taken using kind of PTV measurements, based on the structure detected techniques. Those velocities cannot be captured by the PTV instrument within the liquid jet core, as shown in Figure 5-c, and figures 6-a/6-b. Consequently in the absence of experimental dataset from the centerline of the liquid jet until 100-120 µm, New DNS results were used. Figure 6 displays good agreement between New DNS and Experiments from 100 to 200 µm (figure 6-a) and from 200 to 400 µm (figure 6-b), which set the limits of New DNS validated results. Comparison above upper limits fails to predict dispersed zone flow field mainly due to unsufficient mesh refinement using New DNS. Therefore the available validation range is increased from the centerline up to 700 µm approximately by combining both Experimental and New DNS results. Quantitatively speaking on one hand, figure 6-a clearly exhibits the differences from the centerline of the liquid jet up to 100 µm radially, between the results from ELSA's and New DNS. On the other hand, beyond 100 µm (200 µm, figure 6-b), ELSA tends to underestimate the liquid velocity as compared to New DNS and Experimental results. Such logical results arrive from the formation of tiny droplets beyond 100-200 µm, thus un-resolved scales become relevant as we move outward radially. ELSA-LES + Lagrange model accounts properly for the droplets formation in the dispersed spray zone until certain extent. However, the results presented so far are not conclusive, and they need further research. It is believed when droplets are created, there is a relative velocity between the phases at the interface, instead of an independent flow field for each phase.

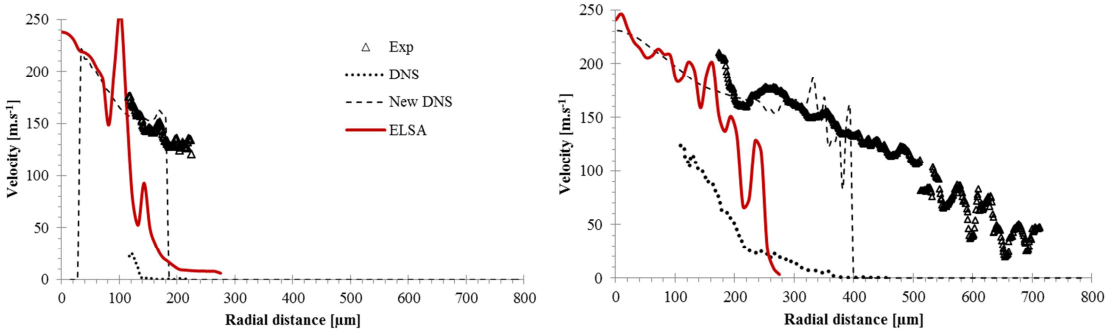


**Figure 6.** Left, liquid velocity located 250 microns from the inlet. Right, liquid velocity located 1500 microns from the inlet.

**Application**

As stated above, FCC risers involved complex physics, such atomization, vaporization and chemical reactions. In this work, we study the atomization process within a FCC injector as displayed in figure 7-a.

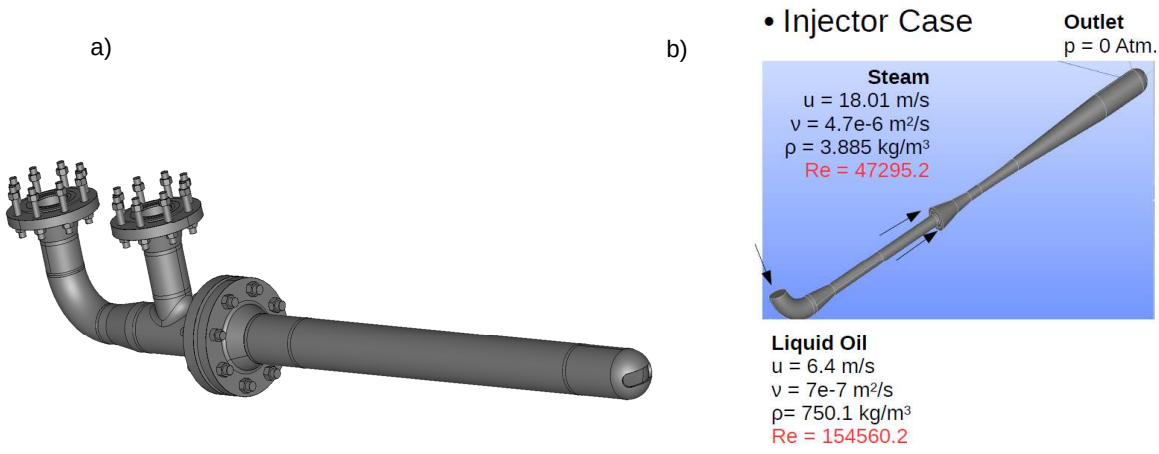


**Figure 7.** a) FCC injector geometry. b) FCC injector model and boundary conditions.

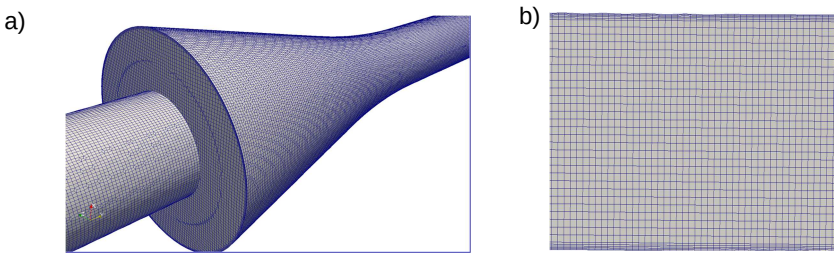


**Figure 8.** a) 3D mesh of the FCC injector. b) Inner cells for the FCC injector model

In figure 7-b it can be seen the boundary conditions applied to the FCC injector model, hence making it suitable for ELSA algorithm based on high Reynolds and Weber numbers. The mesh was done with an open-source library for mesh generation implemented within OpenFOAM® framework, named cfMesh. The library supports generation of meshes of arbitrary cell types, and the currently implemented workflows generate Cartesian type of polyhedral in both 2D and 3D space, tetrahedral and arbitrary polyhedral [19] as exhibited in figure 8-a. In figure 8-b, it is shown the unstructured hexahedral mesh with inflation layers adjacent to the wall, with a total of 5 million cells.

Firstly to evaluate the mesh and get quickly robust and computationally less expensive results than LES, a time-averaging of the governing equations of the Eulerian solver in ELSA was used. Figure 9-a shows, the results of gradients in the Stream-wise direction of the axial velocity which reveals wall-bounded effects in the phase mixing zone, with high gradients near the wall. Phenomena never encountered in ECN injectors. Based on the fact, the FCC injector model was meshed using the same height of the first cell adjacent to wall, in figure 9-b exposes the values of Y+, which indicates that highest velocities in the FCC injector are located near the wall, therefore requiring a more accurate turbulence model with a better mesh quality (sensitivity analysis)

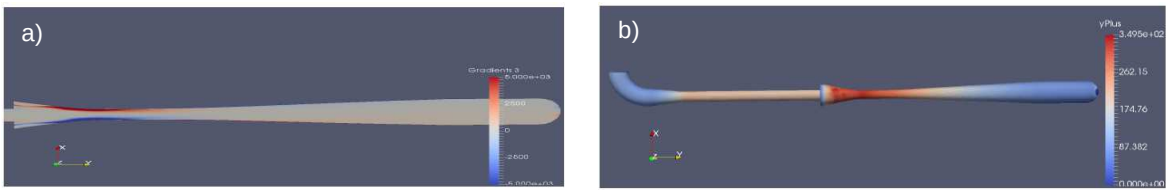


Figure 9. a) Gradients in the Stream-wise direction of the axial velocity. b) yPlus.

Figure 10-a illustrates the liquid volume fraction using an improved mesh and ELSA-LES model without the interface capturing method. The two-phase flow within the FCC injector demonstrates that there is a liquid core flow and annulus gas flow compressed by the latter inside the injector. This concentric behavior pushes the gas to wall, hence increasing its stream-wise velocity near the wall. Figure 10-b shows the velocity profile in the transverse cross-section which verifies the highest velocities near the wall.

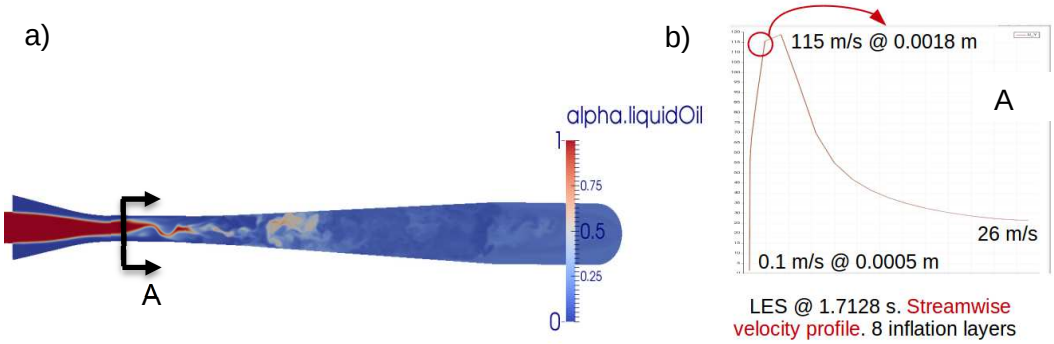


**Figure 10.** a) Liquid Volume Fraction. b) Velocity profile in the 'A' transverse cross-section.

**Conclusions**

An enhanced ELSA-LES model implemented within OpenFOAM® framework was presented. The liquid interface capturing method has been handled a long with the turbulent diffusion liquid flux by a pondered parameter, $C_\alpha$, which depends on the interface resolution and curvature of the interface. Moreover, a Lagrangian approach was studied to account for the spray atomization zone, where droplets are created. Validation has been carried out

based on experimental dataset and DNS simulation. Results have not yet been conclusive due to certain parameter sensitivity when it comes to creating droplets. Authors strongly advise further research in the spray zone as the one being held in our facilities. Having modelled FCC injectors, it has been demonstrated the wall-bounded turbulent effects on the two-phase flow, where the highest velocities are located near the wall, thus increasing the phase mixing.

**Acknowledgements**
This work was partly supported by VINCI TECHNOLOGIES and CNRS. Simulations were carried out at the CRIHAN (Centre de Ressources Informatiques de Haute Normandie) and CINES (Centre Informatique National de l'Enseignement Supérieur).

**Nomenclature**

| | |
|---|---|
| $\mu_{sgs}$ | Dynamic SGS viscosity [Pa s] |
| $\rho$ | Density [$kg/m^3$] |
| Δ | Cutoff width [m] |
| S | Strain rate [1/s] |
| $\tau_{ij}$ | Sub-grid-scale stresses [Pa] |
| $u$ | Velocity [m/s] |
| $p$ | Pressure [Pa] |
| Sch | Schmidt number |

**References**

[1] Sadeghbeigi, R., 2012, Fluid catalytic cracking handbook. *B/H.* 3rd Edition. Chapter #1. Pp. 14-17.
[2] Grace, J. R., 1997, "Circulating fluid beds" ©Chapman & Hall.
[3] Gan, J. Zhao, H., 2011, Numerical simulation of hydrodynamics and cracking reactions in the feed mixing zone of multiregime gas-solid riser reactor. Ind. Eng. Chem. Res. 50 (20), pp. 11511-11520.
[4] Rajesh, P. Dawei, W., 2012, Effect of injection zone cracking on fluid catalytic cracking. American Institute of Chemical Engineers.
[5] Tuyen, T. B. Ngujen, Subhasish M., 2015, Comparison of vaporization models for feed droplet in fluid catalytic cracking risers. Chemical Engineering Research and Design. Elsevier, pp. 82-07.
[6] Qilong, H. and Jinxian, L. 2016, Experiment and Numerical studies on the atomization of a swirl feed nozzle. Journal of Industrial and Intelligent Information, Vol. 4, No. 1.
[7] Theologos, K. N., 1999, Feedstock atomization effects on FCC riser reactors selectivity. Chemical Engineering science 54, pp. 5617 – 5625.
[8] Chesnel, J., 2011, Large Eddy Simulation for atomization: application to automotive engines injection. PhD Thesis, CORIA UMR 6614, Rouen, France
[9] Corrosionpedia, https://www.corrosionpedia.com/definition/120/atomization ([cit. 2016-05-10])
[10] Hecht, N., 2016, Large Eddy Simulation of liquid flow: Spray application. PhD Thesis, CORIA UMR 6614, University of Rouen, France
[11] Davide, Z. Estivalezes, J., L., 2013, Numerical simulation of primary and secondary atomization. C. R. Mecanique 341 15 – 25.
[12] Vallet, A., Borgui, R., 1999, Euler model for liquid jet atomization, Sci. Paris Ser. II b 327, 1015 – 1020.
[13] Lebas, R. Menard, T., Beau, P. A., Berlemont, A., Demoulin, F. X., 2009, Numerical simulation of primary break-up and atomization: DNS and modeling study. Int. J. Multiph. Flow 35 (3), 247 – 260.
[14] Raees, F., Van der Heul, .D. R., 2011, Evaluation of the interface-capturing algorithm of OpenFOAM for the simulation of incompressible immiscible two-phase flow. Department of Applied Mathematical Analysis, Delft, The Netherlands.
[15] Andreini, A. Bianchini, C., Puggelli, S., Demoulin, F. X., 2016, Development of a turbulent liquid flux model for Eulerian-Eulerian multiphase flow simulation, Int, J. Multiph. Flow 81, 88 – 103.
[16] Versteeg, H. K., Malalasekera, W., 2007, "An Introduction to Computational Fluid Dynamics, The finite volume method". Pearson Education.
[17] Hect, N., Reveillon J., Puggelli S. and Demoulin F.X, 2016, Toward a general LES Model for Atomization, 9th International Conference on Multiphase Flow, Firenze, Italy.
[18] Vaudor, G., 2015, Atomisation assistée par un cisaillement de l'écoulement gazeux Développement et validation. Ph.D. Thesis. CORIA UMR 6614, University of Rouen, France
[19] cfMesh, meshing tool, https://www.cfmesh.com/cfmesh/ ([cit. 2016-05-10])